N-Component in Extensive Air Showers†

K. GREISEN, W. D. WALKER,* AND S. P. WALKER*
Cornell University, Ithaca, New York

(Received July 6, 1950)

The high energy N-component, capable of producing penetrating showers, has been found to have an intensity near the cores of air showers about 60 percent as great as that of the non-interacting penetrating particles, and about ½ percent as great as that of the electrons. The ratio of charged to neutral N-component is about 1.5. Large penetrating showers are more frequently observed to be associated with air showers than are small penetrating showers. It is suggested that all of the N-component in the lower atmosphere belongs to extensive showers and contributes to the shower development. Near the core, the lateral density distribution of the N-component is found to be as strong as that of the electrons. It is shown that this results from purely geometric considerations, provided one accepts the concept of a core containing N-component of great energy, continually feeding out lower energy particles to the side.

I. INTRODUCTION

THAT particles with strong nuclear interaction, or N-component, exist in the extensive air showers has already been shown by cloud chamber photographs,[1–3] by Geiger counter experiments on penetrating showers[4,5] and on penetrating particles in air showers,[6–8] and by detection of groups of low energy neutrons produced by penetrating particles in the air showers.[9,10]

The experiment described below was undertaken to add to the quantitative information concerning the N-component of high energy in extensive air showers. The experiment was carried out at Mt. Evans, Colorado; elevation about 4260 meters, mean pressure about 616 g/cm².

The N-component and μ-meson detector consisted of the heavily shielded array of 85 counters shown in Fig. 1. We refer to this below as the PP (penetrating particle) detector. The absorber thickness above trays A_1 and A_2 of the PP detector was varied from 13 inches of lead to zero. In most of the measurements, this absorber was thick enough to prevent electrons of the air showers from reaching tray A. The lower trays were further protected from incident electrons by the other layers of lead and iron.

To detect the air showers, there were two trays of unshielded counters, one situated at 7 meters from the shielded array, and one at 26 meters. In each tray were 5 large counters (usually of area 560 cm² each) and 3 small counters (each of area 29 cm²). For brevity we shall henceforth call the unshielded trays ED (electron density) detectors.

Mixing circuits allowed the selection of events in which at least one of the unshielded counters was struck simultaneously with a preselected minimum number of counters, n, in each of the trays B, C, D of the PP detector. Such a coincidence is called AS (air shower) $+B^nC^nD^n$. The resolving time for this coincidence was about 5 μsec. Thereupon a master pulse was generated, which was put in coincidence with each of the 101 individual counters, with a resolving time of about 30 μsec. An array of neon bulbs was photographed to show which counters had been struck.

During most of the running time, the trigger requirement was $AS+B^2C^2D^2$. For comparatively short times, the requirement was reduced to $AS+B^1C^1D^1$, or to $B^2C^2D^2$ (at least two penetrating particles, but without the requirement that an unshielded counter be struck). The coincidence rate $B^2C^2D^2$ was continually recorded with a mechanical register.

The observation of which counters had been struck in the ED detectors permitted a grouping of the showers according to the electron density at 7 m and at 26 m from the PP detector. The simultaneous use of counters of two sizes provided a rather wide range over which the density could be roughly determined.[11]

II. EXAMPLES AND INTERPRETATION OF COMMON EVENTS

Figures 2A to 2D show illustrations of some of the types of events recorded with the trigger $AS+B^2C^2D^2$. In these drawings we have blackened the circles representing the counters struck in the PP detector.

In general, we interpret a coincidence of the type $AS+B^2C^2D^2$ as a penetrating shower associated with an air shower, unless the counters struck in the PP detector are so located as to indicate parallel particles arriving from the air, or a single particle strongly inclined rela-

† Some of the apparatus used in this experiment was made available through a contract with ONR.

* Now at Rice Institute, Houston, Texas.

[1] W. B. Fretter, Phys. Rev. **76**, 511 (1949).
[2] J. Ise, Jr., and W. B. Fretter, Phys. Rev. **76**, 933 (1949).
[3] W. W. Brown and A. S. McKay, Phys. Rev. **76**, 1034 (1949).
[4] J. Tinlot and B. Gregory, Phys. Rev. **75**, 520 (1949).
[5] K. Sitte, Phys. Rev. **78**, 721 (1950).
[6] Cocconi, Tongiorgi, and Greisen, Phys. Rev. **76**, 1020 (1949).
[7] B. Chowdhuri, Proc. Phys. Soc. **A63**, 165 (1950).
[8] G. T. Zatsepin and L. E. Sarycheva, Dokl. Akad. Nauk. SSSR **69**, 635 (1949).
[9] V. Cocconi Tongiorgi, Phys. Rev. **74**, 226 (1948); **75**, 1532 (1949).
[10] G. Cocconi and V. C. Tongiorgi, Phys. Rev. **79**, 730 (1950).

[11] During the experiment, the larger counters in the ED were changed from 560 to 196 cm² each, which necessitates an extra subdivision of the data given below. The reason for the change was a rapid deterioration of the large counters which finally made it impossible to continue their use. We do not believe these troubles introduce significant unreliability in our data, since we tested the counters frequently, replaced bad ones, and discarded all data taken with questionable counters.

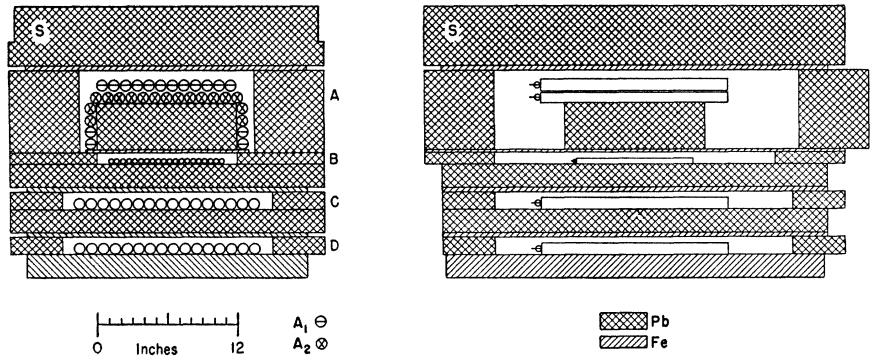

FIG. 1. Cross sections of the *PP* detector. The thickness of the absorber above the top tray, *A*, was varied from 13 inches of lead to zero.

tive to the zenith. The first question we must decide is whether or not a large fraction of these events could be due to other phenomena.

A. Electrons and Photons Penetrating through the Lead

We shall give primary emphasis to the data taken with 5 to 13 inches of lead (plus $\frac{3}{8}$ inch iron) above tray *A*. Between trays *A* and *B* was another 4 inches of lead (and $\frac{1}{4}$ inch iron). As shown in Fig. 1, the 4-inch absorber between *A* and *B* did not completely cover the ends of trays *C* and *D*, which were wider than *B*. However, between tray *B* and the lower trays were two broad layers of absorber, so that even the ends of tray *C* were covered in the vertical direction with 7 to 15 inches of lead plus an inch of iron. With the maximum absorber in place (i.e., for about half of our data), the lowest tray, *D*, was covered with 57 cm of absorber over most of its area, and 47 cm over the ends.

The side and end shielding was about 6 inches of lead. Since only badly scattered particles (i.e., those of low energy) travel horizontally, the effective thickness for particles from the side was considerably more than 6 inches. Moreover, showers from the side could be recognized in the hodoscope records.

It is essential that it be accepted that electron showers incident from the air could not penetrate to all the counter trays except with negligible frequency, and that even the penetration to trays *B* and *C* be rare. According to our previous experiments and calculations,[12,13] we believe the absorber thicknesses were more than sufficient to assure this.

Indeed, even when no lead was above tray *A*, the bottom tray was protected in the vertical direction over most of its area by 8 inches of lead plus an inch of iron, and over the edges by 4 inches of lead plus an inch of iron. Therefore, even in this case, the background effects due to penetration of electrons and photons are expected to be small compared with the rates of the penetrating showers that were recorded.

Further guarantee that electrons and photons penetrating the lead were unimportant is given by the dependence of the rate $AS+B^2C^2D^2$ on the thickness of lead above the top tray (Table I).

B. Cascade Showers Generated by Single Mesons

The knock-on and radiation processes of mesons could produce a serious background if the mesons were as abundant, compared with the *N*-component, as in the cosmic rays not associated with dense air showers (see the following paper). However, associated with extensive air showers we observe the penetrating showers to be almost as frequent as the single penetrating particles. Therefore the small probabilities of mesons to produce multiple knock-ons or high energy cascade showers are negligible.

C. Inclined Mesons

A single meson travelling in a strongly inclined direction could strike two counters in each of the trays *B*, *C*, *D*. It would then either miss tray *A* or strike one of the side counters of the tray. Some events of this sort did occur, but they were easy to recognize and eliminate (see Fig. 2D). In almost every case only one of the unshielded counters was struck, indicating that these were chance coincidences of single mesons with unassociated particles striking an unshielded counter.

D. Chance Coincidences

Because of the high counting rate in the unshielded counters (430/sec. in each *ED* detector), there was a significant probability that a penetrating shower should be coincident by chance with an unassociated discharge of a single counter in one of the two unshielded sets. This probability was approximately 0.003 per *ED* detector or 0.006 for both trays when the larger counters were used, and 0.0025 for both trays when the smaller counters were used. The chance coincidence rate was about 20 percent of the coincidence rate observed for penetrating showers and single unshielded counters. The chance coincidences with showers striking more than one counter in an *ED* detector were negligible.

These facts are verified by the observation (see Figs. 4 and 6) that the frequency of coincidences between penetrating showers and particles in the *ED* at 7 meters was much greater than that of coincidences with the *ED* at 26 meters.

[12] Cocconi, Tongiorgi, and Greisen, Phys. Rev. **75**, 1063 (1949).
[13] K. Greisen, Phys. Rev. **75**, 1071 (1949).

In addition to the background effects listed above, there are other sources of error which affect our conclusions concerning the point in the absorber at which the penetrating shower begins, whether the penetrating shower is initiated by a charged or neutral particle, or whether non-interacting particles are present in addition to one or more penetrating showers. These uncertainties arise mainly from the ejection of secondary particles backwards or to the side, and from successive interactions occurring in a single penetrating shower. However, these errors do not lead to false indication that a penetrating shower has occurred.

III. ANALYSIS OF EVENTS RECORDED WITH THE TRIGGER $AS+B^2C^2D^2$

The pictures showing air showers plus two or more penetrating particles were examined and subdivided into the following classes:

(1) Side showers: penetrating showers or mesons coming from the side, so as to strike the side counters of tray A or miss tray A altogether. These events are excluded as being outside the solid angle in which particles are accepted.

(2) Parallel tracks of penetrating particles: we list the number of events of this type, not the number of tracks.

(3) Penetrating showers starting in the absorber above tray A.

(4) Penetrating showers starting in the "producing layer" between trays A and B. Type 4 was further subdivided according to whether the primary particle initiating the shower appeared to be neutral or charged.

Table II presents this subdivision of the data for three thicknesses of absorber above tray A.

One cannot deduce "mean free path" values from the data of Table II, for the following reasons: (a) when the absorber was 5 inches Pb, electrons could penetrate as far as the counters of tray A, and make showers appear to start above this tray when in reality they started below it; and (b) layers of absorber added on top are not as efficient in producing detectable showers[14] as the layers below tray A, because of the absorption of the secondaries and because of the smaller solid angle subtended by the lower trays at the point of origin of the shower. Both of these effects tend to reduce the variation of the ratio of PS produced below A to PS produced above A, as the absorber is increased.

Nevertheless, the observed decrease of the ratio PS produced below A to PS produced above A, as the absorber is increased, helps to verify that most of the apparent penetrating showers were not caused by μ-mesons, because mesons that can produce penetrating cascades or multiple knock-ons should not be appreciably absorbed in 8 inches of lead.

One can derive an approximate ratio of mesons to N-component in the air showers from the frequency of parallel tracks compared with that of penetrating showers. Let M and N represent the numbers of mesons and N component relative to the total number of charged particles in the showers, and let Δ represent the shower density. Then, assuming that the mesons and nucleons are distributed in constant proportion to the electrons, the frequency of observation of pairs of mesons is given by:

$$K\int_0^\infty \tfrac{1}{2}(MS\Delta)^2 e^{-MS\Delta}\cdot e^{-NS\Delta}(1-e^{-S'\Delta})\Delta^{-\gamma}d\Delta.$$

Here S is the area of the shielded counters and S' the area of the unshielded counters. The term $\exp(-NS\Delta)$ enters because two parallel tracks could not be observed in the presence of a penetrating shower. The term $[1-\exp(-S'\Delta)]$ is the probability that the unshielded tray be struck.

TABLE I. Dependence of the rate $AS+B^2C^2D^2$ on the lead absorber above the top tray.

Absorber above tray A	Rate (min.$^{-1}$) $AS+B^2C^2D^2$
5″ Pb, 148 g/cm^2	0.155±0.010
9″ Pb, 260 g/cm^2	0.130±0.005
13″ Pb, 370 g/cm^2	0.114±0.004

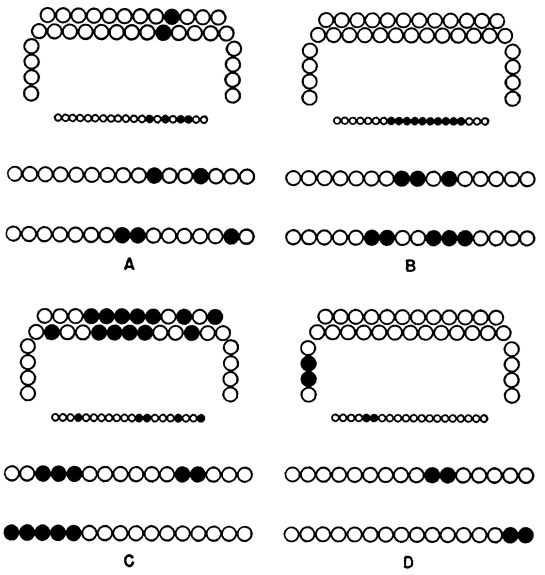

FIG. 2. A. Small penetrating shower initiated in the "producing layer" beneath tray A by a single ionizing particle. Two unshielded counters were struck at 7 meters distance, and none of 26 meters. The lead above tray A was 13″ thick. B. Penetrating shower initiated in "producing layer," under 13″ Pb, by a neutral particle. Two unshielded counters were struck at 7 m and one at 26 m. C. Penetrating shower of a kind seen more frequently than the types in Figs. 2A and 2B. It was initiated in the 13″ Pb above tray A, but further multiplication apparently occurred beneath tray A. One cannot trace the paths of individual particles. D. Most frequent spurious event, caused by single meson from the side. In practically all cases of this sort, only one of the unshielded counters was struck. These events are probably chance coincidences of mesons with unassociated particles in the air, rather than real associations of mesons with air showers.

[14] E. P. George and A. C. Jason (1950). We are grateful to the authors for communicating their results prior to publication.

TABLE II. Subdivision of events with trigger requirement $AS+B^2C^2D^2$.

Absorber above tray A	Side showers	Parallel tracks	PS starting above A	PS in producing layer: Neutral primaries	PS in producing layer: Charged primaries	Ratio: $\frac{PS \text{ below } A}{PS \text{ above } A}$
5″ Pb 148 g/cm²	62	5	181	19	29	0.265±0.043
9″ Pb 260 g/cm²	109	3	386	27	53	0.207±0.025
13″ Pb 370 g/cm²	227	10	716	34	78	0.156±0.016
Totals	398	18	1263	80	160	

With the same notation, the frequency of observed N-component is

$$K\int_0^\infty (1-e^{-NS\Delta})(1-e^{-S'\Delta})\Delta^{-\gamma}d\Delta.$$

By using the approximation that S' is large compared with MS and NS, one can reduce the ratio of the above integrals to:

$$\frac{\text{Double mesons without } N \text{ component}}{N \text{ component}} = \frac{\gamma-2}{2}\frac{M^2}{N(M+N)^{3-\gamma}}\left(\frac{S}{S'}\right)^{\gamma-2}.$$

This ratio is much more sensitive to the ratio M/N than to the quantity $(M+N)$. In Table II we see that the number of cases of parallel tracks is 1.2 percent of the number of penetrating showers. With[15] $\gamma=2.4$ and $M+N=0.005$ to 0.02, we find $M/N=1.5$ to 1.0.

The above calculation oversimplifies the physical situation and does not take into account correctly the imperfect efficiencies of detecting both the mesons and the N-component. However, the result is correct in order of magnitude, and shows that the high energy N-component is almost as abundant as the mesons in the air showers. A second derivation of the ratio M/N from other data will be given below; it leads to a value somewhat higher (about 1.7) but in reasonable agreement with the above estimate.

IV. RELATIVE NUMBERS OF NEUTRAL AND CHARGED PARTICLES

Only the showers beginning below tray A can be separated according to the sign of the initiating particle. The total number of apparently neutral-primary events is 80, and of charged-primary events is 160, so that it appears at first glance that the neutral N-component is $\frac{1}{3}$ of the total.

However, it is known from other experiments[16] that when a neutron produces a penetrating shower, a back projected particle frequently makes it appear that the primary was charged. Also, in a small percentage of the events the neutral particle that produces a penetrating shower will be accompanied in the air shower by an independent charged particle. Similarly, a fraction of the showers produced by charged particles will be missed because back projected secondaries or accompanying particles make it appear that the shower began above tray A instead of below. The net result of these effects is to increase the apparent ratio of charged to neutral primaries.

From the recognizable cases in the hodoscope records, and from the data of Walker[16] and other unpublished information, we have estimated the corrections, with the result that the ratio of charged to neutral particles is 1.5±0.3. The error listed includes an estimate of the uncertainties in the corrections, as well as the statistical error.

V. RELATIVE NUMBERS OF μ-MESONS AND N-COMPONENT

A better evaluation of the relative numbers of μ-mesons and N-component can be made from the pictures taken under the trigger requirement of $AS+B^1C^1D^1$, when single penetrating particles as well as penetrating showers could be seen.

In order to reduce the effects of chance coincidences we consider only the events in which two or more of the unshielded counters were struck. Even with this restriction of the data, a large fraction (about 40 percent) of the cases of "single mesons plus air showers" are casuals.

The use of the criteria for discriminating between mesons and N-component is illustrated by the data of Table III, where the pictures have been classified according to the thickness of lead above tray A and the multiplicity of counters struck in rows B, C, and D.

In examining Table III, we see that class 5 (penetrating showers) is about half of class 1 (mostly mesons) independently of the thickness of lead. This independence can be explained by the long range of the energetic penetrating showers.

Class 2 is 25 percent of the sum of classes 1 and 2. If both of these classes represent single penetrating particles, a knock-on probability of 8 percent per layer of absorber is indicated. This is in close agreement with the value of 7 percent reported by Brown, McKay, and Palmatier,[17] and indicates that almost all the events of class 2 should be considered as single penetrating particles that generate knock-on electrons, and not as nuclear disintegrations.

Classes 3 and 4 contain too many events (9 percent of the penetrating particles) to be entirely due to double knock-ons and the small fraction of the knock-on secondaries that can penetrate 2″ Pb plus $\frac{3}{8}$″ Fe. Some of them must represent penetrating showers either of

[15] J. Treat and K. Greisen, Phys. Rev. **74**, 414 (1948).
[16] W. D. Walker, Phys. Rev. **77**, 686 (1950).
[17] Brown, McKay, and Palmatier, Phys. Rev. **76**, 506 (1949).

small size or starting below tray B. These events are few enough so that precision is not needed in the assignment. We estimate that $\frac{1}{3}$ of them are due to electronic secondaries of single penetrating particles, and $\frac{2}{3}$ are due to energetic nuclear disintegrations.

Thus, we have a total of 96 recognized arrivals of N-component and 220 single penetrating particles. To these numbers the following corrections must be applied:

(1) Chance coincidences account for about 85 of the cases of single penetrating particles plus air showers.

(2) Failure of the N-component to interact in the absorber above tray B makes 7 percent of the charged N-component appear as single penetrating particles, and 7 percent of the neutral N-component fail to be recorded at all.

(3) Single mesons are apt to be missed in the presence of a penetrating shower. By using the approximate meson and N-component intensities relative to the electrons, and integrating over the density spectrum of showers that strike the ED detectors, we find that 9 percent of the mesons were probably accompanied by N-component and therefore escaped observation.

(4) Although strongly inclined penetrating showers were eliminated by examination of the hodoscope records, the effective area for detection of the N-component was nevertheless greater than the effective area for single mesons, because of the spread of penetrating showers and because the "producing layer" between trays A and B was larger in area than tray B (144 sq. in. as compared with 100 sq. in. for tray B). We estimate the correction as 20 percent plus or minus 10 percent.

After applying these corrections, we have for the ratio of N-component (including both charged and neutral N-component) to mesons in the air showers,

$$N/M=0.60\pm0.15.$$

The uncertainty we have listed includes both the statistical standard error and the estimates of uncertainties in the corrections. Sitte[5] has obtained a considerably lower value for the ratio N/M, 0.26 ± 0.03, which seems inconsistent with the data analyzed in the present section, and with the data analyzed above in Section III, where we found $N/M=0.8\pm0.2$. His measurements were made at an altitude 1000 meters lower than the present ones, but the chief cause of the discrepancy probably lies in a difference in the energy and geometric requirements imposed on the recorded nuclear interactions.

VI. COMPARISON OF PENETRATING SHOWERS ASSOCIATED AND NOT ASSOCIATED WITH AIR SHOWERS

The penetrating showers observed both associated and not associated with air showers have been classified according to size, as indicated by the number of counters struck in the lowest row, D. The relative frequencies are shown in Fig. 3, with the associated and non-associated events normalized to be equal in number for the smallest showers, that struck only two counters in row D. The total number of counters in row D was 16.

TABLE III. Classification of events seen with trigger $AS^2+B^1C^1D^1$.

Pb above tray A	5″	9″	13″	Totals
Class 1: Single particles with no secondaries observed in either of the rows B, C, D	25	76	59	160
Class 2: Single particles with secondary observed in one row only	8	26	20	54
Class 3: Secondary observed in row B and row D but not in row C	0	5	2	7
Class 4: Secondary observed in two adjacent rows	1	3	8	12
Class 5: Penetrating showers, recognized by multiplicity in all 3 rows, or by high multiplicity (4 or more) in 2 rows	13	43	27	83

The difference between the two histograms shows that the large penetrating showers are more often associated with dense air showers than are the small penetrating showers.

This is also illustrated by the data presented in Table IV, where we compare the fractions of the penetrating showers that are associated with observed air showers, for all penetrating showers that strike two or more counters in row D, and for the showers that strike seven or more counters in row D. It may be seen that a comparatively large fraction of the big penetrating showers are associated with observable air showers.

Occasionally, huge penetrating showers or groups of such showers occurred that discharged all or almost all of the 85 counters of the PP detector. In every such case, an accompanying air shower was detected.

These results support the view that all of the N-component is associated with extensive air showers, but that the particles of higher energy are more apt to be found near the core or in a shower of great density, than are the particles of lower energy.

VII. DISTRIBUTION OF DENSITIES OF RECORDED AIR SHOWERS ACCOMPANYING PENETRATING SHOWERS

For each event of the type $AS+B^2C^2D^2$ an approximate shower density measurement was made at 7 m and at 26 m from the PP detector, on the basis of the number of unshielded counters struck. By following an analysis similar to that of Cocconi, Tongiorgi, and Greisen,[6] and using the data of Treat and Greisen on Mt. Evans[15] for the *a priori* probabilities of showers of different densities, most probable and median densities were calculated for the different counter combinations, which were then grouped into density classes as listed in Table V. For the extreme classes the probability distributions are not very steep so that individual events may differ from the most probable or median density by a rather large factor, but for the other classes the error in an individual density assignment should seldom be more than a factor three.

The experimental results did not seem to be sensitive

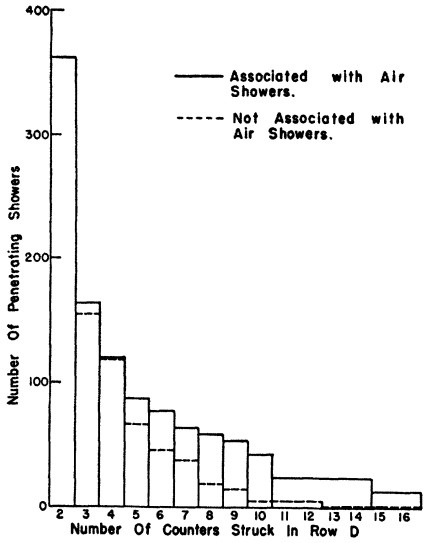

FIG. 3. Distribution of penetrating shower sizes as indicated by number of counters struck in the lowest counter tray, D. The non-associated showers, represented by the dashed line, have been normalized to the associated showers at $D=2$, by multiplying the observed number of local events by a factor 1.36. Both histograms include showers beginning above tray A as well as below tray A.

to the amount of absorber used; therefore in Fig. 4 we have put together the data obtained with 5″, 9″, and 13″ Pb above tray A. Figure 4 lists the numbers of cases falling into the various density classes at the two *ED* detectors. For all of these data the unshielded counters in each *ED* detector consisted of 5 counters of 560 cm² each, and 3 of 29 cm² each.

Chance coincidences and showers or mesons coming from the side were not removed from the tabulation in Fig. 4, but occur almost entirely in the groups 0—I and I—0; i.e., coincident with only a single counter pulse in one of the *ED* detectors. It may be noted that such coincidences were more than twice as frequent with the *ED* at 7 m as with the *ED* at 26 m, showing that only a small fraction of the showers detected at 7 m were casuals. On the other hand, we know from the resolving time of the circuit that a large fraction (about 200 cases in Fig. 4) of the events in which no counter was struck at 7 m and only one was struck at 26 m were chance coincidences. Of the more dense showers, a negligible number were casuals.

From the data of Fig. 4, the integral density distributions were derived that are shown in Fig. 5. In drawing these curves it was assumed that half of the showers in each density class had densities above the calculated median density for that class, and that the remainder had densities above the median density of the next lower class. This should be true in first approximation for all the classes appearing in the graph. Class 0 and half of class I are not included; and class I has been corrected for the chance coincidences.

The curves represent the frequencies of extensive showers that (a) are associated with a recorded penetrating shower, (b) strike the *ED* detector with at least one particle, and (c) have a density greater than the corresponding abscissa. As the density decreases below 10 particles/m², an increasing fraction of the associated air showers miss the *ED* detectors entirely. If this did not occur, the curves would continue to rise with decreasing density, as shown by the dashed extension of the "calculated distribution."

For comparison with the data, a theoretical curve has been included in Fig. 5, representing the *a priori* probability distribution of recorded showers of density greater than Δ. This is given by:

$$F(\Delta)=243\int_{\Delta}^{\infty}\delta^{-2.4}d\delta[1-\exp(-S'\delta)]\times[1-\exp(-NS\delta)]\text{ per min.}$$

Here the first term in brackets represents the probability that an unshielded counter be struck, and the second term in brackets is the probability that N-component hits the *PP* detector. The coefficient 243 (per minute) was taken from the counting rates of Treat and Greisen;[15] the areas S and S' were taken as 0.065 and 0.27 meter respectively; and for N, the number of penetrating shower producers per electron, the value 1/200 was assumed.

The assumption of perfect correlation between N-component and electron densities, which is implicit in this equation, means that the curve should be most nearly correct for an *ED* detector at zero meters from the *PP* detector.

The agreement in shape between the calculated and experimental curves is satisfactory. The absolute values on the calculated curve are higher than the measured values, but there are several reasons for this to be so, even if our estimate of the ratio between N component and electron density is correct. First, there is the 7-meter separation between the N-component detector and the nearer *ED* detector, which accounts for about 30 percent loss in counting rate, if the N-component is distributed similarly to the electrons.[12] Secondly, there is the inefficiency of the N-component in causing coincidences of the type $B^2C^2D^2$ (see Section V above). This is accentuated by the fact that most of the data in Figs. 4 and 5 were taken with 9″ or 13″ Pb above tray A, and the average rate was 22 percent lower than the rate under 5″ Pb. Therefore one should expect the experimental data to fall lower than the calculated curve by a factor of 0.4 to 0.5, about as observed.

Hence we conclude that the amount of high energy N-component relative to the electrons is about 0.005, as assumed in the calculations. We believe this to be correct within 40 percent. The uncertainty in the lower energy limit of the detected N-component makes higher precision scarcely meaningful. It must be emphasized that this relative intensity was determined only near the cores of the air showers, and may be quite different from the relative intensity of nucleons and electrons far from

TABLE IV. Penetrating showers associated and not associated with observed air showers. Rates corrected for casuals and events from the side.

$B^2C^2D^2$	3.23 ±0.15 min.$^{-1}$
$AS+B^2C^2D^2$	0.102±0.005 min.$^{-1}$
Ratio	3.2 percent
$B^2C^2D^7$	0.34 ±0.04 min.$^{-1}$
$AS+B^2C^2D^7$	0.031±0.002 min.$^{-1}$
Ratio	9 percent

the core. Moreover, it applies to both charged and neutral N-component.

In Section V we found that the N-component was about 60 percent as numerous as the μ-mesons. This would indicate that the meson intensity relative to the electrons is about 0.008 near the shower core, and the total penetrating component (detectable by its own charge or by producing charged secondaries) amounts to 1.3 percent of the electrons. This is in agreement with other measurements at a slightly lower elevation.[6,12] The measurement of Treat and Greisen[15] gives a higher number, partly because they used insufficient absorbers and partly because of a difference in distance from the cores of the showers (see discussion by Ise and Fretter[2]).

Data similar to those of Figs. 4 and 5 were also taken with zero absorber above the counter tray A, and with 10″ or 17″ of graphite. For these data, another change was a reduction in area of the larger counters from 560 to 196 cm^2. Therefore a smaller number of low density showers were detected and there were also less chance coincidences. The densities corresponding to the various counter combinations are listed in Table V, and the data are collected in Fig. 6. Graphs of the density distributions are in Fig. 7, where the dashed curve represents a distribution calculated in the same way as the one in Fig. 5.

The experimental ordinates in Fig. 7 are higher than in Fig. 5, agreeing more closely with the calculated curve. This is due partly to increased efficiency and smaller absorption in the detector, and partly to the inclusion of some events caused by high energy electrons and photons.

When the absorber above tray A was entirely removed the upper row of 12 counters in tray A could be

TABLE V. Median densities for the density classes in Figs. 4, 6, and 8.

Density class	Median density; classes in Fig. 4	Fig. 6 and classes at 7 m in Fig. 8	Classes at 0 m in Fig. 8
0 (no counter struck)	0	0	2 m^{-2}
I (one counter struck)	1.25 m^{-2}	3 m^{-2}	8
II	6	16	18
III	14	36	35
IV	25	66	75
V	50	120	150
VI	100	250	250
VII	250	1100	600
VIII	1000	—	—

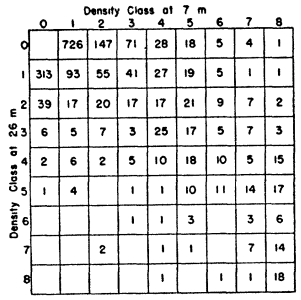

	0	1	2	3	4	5	6	7	8
0		726	147	71	28	18	5	4	1
1	313	93	55	41	27	19	5	1	1
2	39	17	20	17	17	21	9	7	2
3	6	5	7	3	25	17	5	7	3
4	2	6	2	5	10	18	10	5	15
5	1	4		1	1	10	11	14	17
6				1	1	3		3	6
7			2		1	1		7	14
8					1		1	1	18

FIG. 4. Density distribution of air showers at 7 m and at 26 m from the PP detector, for 1974 events of type $AS+B^2C^2D^2$. Absorber above tray A in PP detector = 5″, 9″ or 13″ Pb. The median densities for the different classes are listed in Table V.

used for the density measurement. Always one of the counters struck was discounted, as being due to the primary particle initiating the penetrating shower. This could be sometimes an overcorrection, if the penetrating shower was initiated by a neutral particle, and sometimes an undercorrection, when back-projected particles of the penetrating shower strike the upper counters. The back scattering of electrons from the absorber underneath the counters also tends to increase the apparent shower density. However, we believe that such events in general only change the number of counters struck by plus or minus one, and do not change the order of magnitude of the measured density.

The density classes corresponding to different numbers of counters struck in the top row of tray A are listed in Table V, and the results of the density measurements are collected in Figs. 8 and 9, where the densities at zero and 7 meters are compared. The density class 0 at 7 m had to be blank because the master pulse only occurred when one counter was struck in either the ED

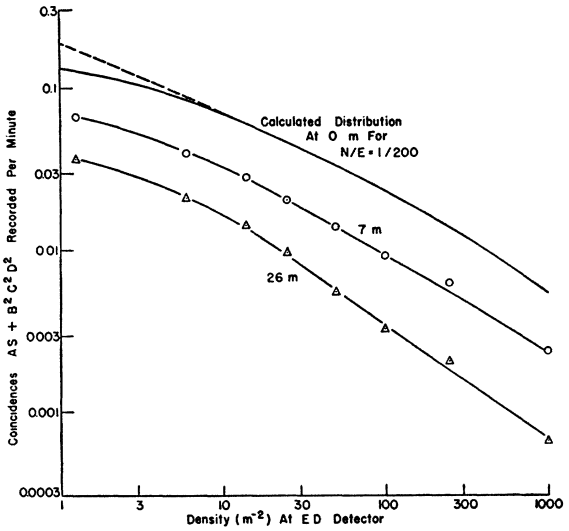

FIG. 5. Integral density distribution of the air showers detected at 7 m and 26 m from the PP detector, in association with penetrating showers. Lead above tray A in PP detector = 5″, 9″ or 13″. The calculated curve is explained in the text.

Density Class at 26 m \ Density Class at 7 m	0	1	2	3	4	5	6	7
0		203	55	19	14	7	6	
1	63	24	13	20	8	5	12	1
2	7	5	6	7	5	8	13	2
3	2		3		2	8	3	2
4	2	1			1	2	14	7
5							5	6
6	1						4	10
7						1	2	15

FIG. 6. Density distribution at 7 m and 26 m, for 594 events of type $AS+B^2C^2D^2$, observed with zero absorber, or 10″ or 17″ graphite, above tray A in the PP detector. The density classes are explained in Table V.

detector at 7 m or the one at 26 m. The few instances in which a counter was struck at 26 m and none at 7 m were mostly chance coincidences.

The requirement for each recorded event, of a particle at 7 m as well as a penetrating shower at the PP detector, increases the *a priori* probabilities of the low density showers so much that even when no counters were struck in tray A the probable air shower density was finite at the PP detector. Except for the groups 0 and I, however, the density classes at zero and 7 m are approximately equivalent (see Table V).

For the data in Figs. 8 and 9, like those in Figs. 6 and 7, the rates probably include some showers due to incident electrons and photons, and are therefore slightly too high.

VIII. SPATIAL DISTRIBUTION

Figures 4 to 9 contain information on the spatial distribution of the N-component in extensive air showers.

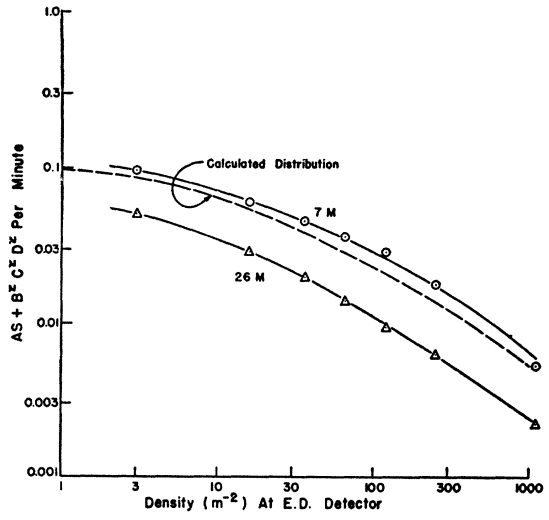

FIG. 7. Integral density distribution of air showers detected at 7 m and 26 m from the PP detector, in association with penetrating showers. Absorber above tray A in PP detector = zero, 10″ or 17″ graphite.

In Figs. 4, 6, and 8, where the data are presented in tabular form, one can see evidence of a correlation between the shower densities measured at the two different distances. The spread of the data, or lack of perfect correlation, is due in part to the errors in the density measurements (which are only expected to be accurate within a factor of 3, or $\pm 1\frac{1}{2}$ density classes), and in part to the cores of the air showers striking at different distances from the apparatus. In the great majority of the events, however, the showers are more dense at 7 m than at 26 m from the PP detector, and more dense at 0 m than at 7 m.

In Figs. 4 and 6 together (excluding the cases in which all of the counters were struck at both ED detectors, and correcting for chance coincidences in classes 0—I and I—0), we find that there are 1629 events (78 percent) in which the density at 7 m seems to be greater than at 26 m, 178 events (9 percent) in which the densities seem about equal, and only 288 cases (14 percent) in which the density at 26 m seems greater than at 7 m. In Fig. 8 (excluding class 0 at each detector and the cases when all the counters were struck at both detectors), we find that there are 115 cases (74 percent) in which the density at the PP detector seems to be greater than at 7 m, 22 events (14 percent) in which the densities are about equal, and only 18 events (12 percent) in which the density at 7 m seems to be greater than at the PP detector.

The average differences in shower density at the two ED detectors can be obtained from the horizontal separations of the frequency-density curves in Figs. 5, 7, and 9. In Figs. 5 and 7, the horizontal separation is found to be a factor varying from about 4 to 6. Because the statistical accuracy and the conditions of measurement were better for Fig. 5 than for Fig. 7, we estimate that the showers were on the average $4\frac{1}{2}$ times as dense at 7 m as at 26 m. From Fig. 9 we conclude that the showers were on the average $3\frac{1}{2}$ times as dense at the PP detector as at 7 m.

According to the Molière theory of the lateral distribution of the electrons,[18] the electron densities at 7 m and 26 m from the cores of air showers at Mt. Evans (where the characteristic scattering length is 130 m) should be in the ratio 5.6 to 1, not much more than the ratio $4\frac{1}{2}$ deduced above. A ratio of 3.5 should exist between the densities at 2.5 m and at 7 m from the core. We conclude therefore that when a penetrating shower *and* an associated air shower were recorded, the core of the air shower was usually very close to (within 5 to 10 meters of) the N-component detector.

Another way of looking at the data is as follows. Air showers of any given density strike both of the ED detectors (in either of the pairs considered above) with the same frequency, and they strike with the core nearer to the detector at 26 m just as frequently as with the core nearer to the other ED detector. But a much larger

[18] G. Molière, in *Cosmic Radiation*, edited by W. Heisenberg (Dover Publications, Inc., New York, 1946).

fraction (by a factor of about 6) of the showers that strike nearer the 7-m *ED* detector exhibit N-component at the *PP* detector, than of the showers that strike nearer to the 26 m *ED*. And a much larger fraction (again by a factor 6) of the showers that strike closer to the *PP* detector than to the *ED* at 7 m exhibit N-component, than of the showers that strike closer to the 7 m *ED*.

This is illustrated by the diagram in Fig. 10. The two circles enclose the areas in which the cores may strike, with the electron density more than about twice as great at one *ED* detector as at the other. The showers falling in one of the circles have N-component detected about 6 times as frequently as the showers falling in the other circle. The average distances (obtained by averaging r^{-1}) of points in the two circles from the *PP* detector are about 6 meters for the nearer, more efficient circle, and 30 meters for the other. Thus, the mean density of the N-component at 6 m from the core is about 6 times as great as at 30 m from the core of an air shower.

A similar treatment of the data of Fig. 8, with *ED* detectors at the *PP* detector and at 7 m, indicates that the N-component density at about $3\frac{1}{2}$ meters from the core is roughly 6 times as great as at about 10 meters. This factor may be slightly exaggerated because of the back scattering effects discussed above.

It is clear that the number of N-component particles per unit area decreases very rapidly with increasing distance from the cores of the air showers: about as rapidly as r^{-1}, or perhaps a little faster. This means that the N-component is concentrated near the shower cores about as strongly as are the electrons.

Cocconi and Tongiorgi, in further studies of neutrons in air showers[10] find that the neutron producers are concentrated near the core about as strongly as the electrons. Presumably the neutron producers are mostly neutrons of higher energy, identical with star producers, and have a mean energy of a few hundred Mev. Thus our conclusion concerning the spatial distribution of the high energy N-component (penetrating shower producers) applies also to the N-component of lower energy.

Cocconi, Tongiorgi, and Greisen[6] have used a group of shielded counters and an unshielded counter as a "core selector" in a study of air showers. The sharp decoherence curves of the core selectors, and the fact that the electron density decreased with distance from the core selector according to the Molière function, and without showing inversions, indicate that the core selectors were much more selective of the cores of showers than were the groups of unshielded counters (*ED* detectors) used in the same experiment. Thus, whatever the particles were that triggered the core selectors, they must have been concentrated in the shower cores more strongly than the low energy electrons. From our present experiment, we must conclude that a large fraction (25 to 50 percent) of the coincidences in the core selectors were due to stars and penetrating showers produced by particles of the N-component in air showers. Hence that experiment also gives evidence for a strong concentration of the N-component near the core. The energy requirement was less than in the present experiment, since the secondary particles did not need to be very penetrating.

Density Class at Om. \ Density Class at 7 m.	0	1	2	3	4	5	6	7
0		45	9	1	1	1		
1		11	5	2				
2		10	2	1	1	1		
3		12	5	1	1			
4		19	3	5	5			1
5		3	5	2	1	3	5	
6		3	2	3	2			1
7		6	4	3	5	7	15	15

FIG. 8. Density distribution of air showers at 0 m and 7 m, for 227 events of type $AS+B^2C^2D^2$, observed with zero absorber above tray A. The upper row of counters, A_1, was used for the density measurement. The density classes are explained in Table V.

One should remember that, both for electrons and for other particles in the showers, the mean distance of the particles from the core is much larger than the mean distance between shower *detectors* and the core, when the detectors require more than one particle; but is equal to the mean distance between detector and core if single particles of the showers are counted. For instance, the mean distance of electrons from the cores of air showers is theoretically about 80 meters (at 3000 m elevation), but the same theory, as applied by Ise and Fretter,[2] shows that showers in which electrons discharge 3 neighboring counters strike mostly within 10 meters of the counters.

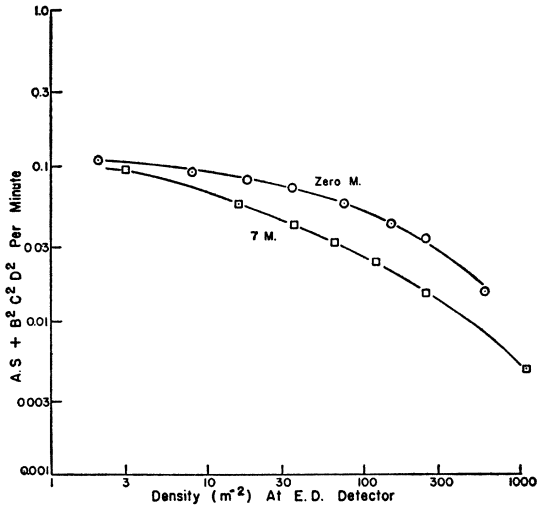

FIG. 9. Integral density distribution of air showers detected at 0 m and 7 m from the *PP* detector, in association with penetrating showers. Absorber above tray A in *PP* detector = zero.

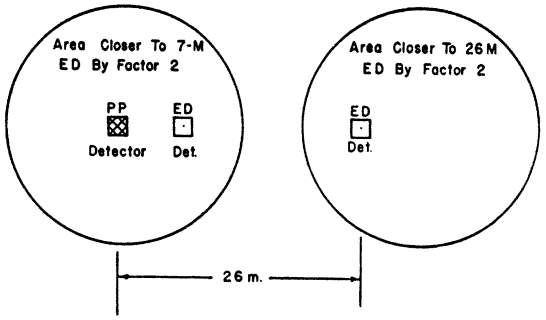

FIG. 10. Diagram illustrating discussion of spatial distribution of the penetrating particles in air showers. The showers with cores falling in one of the circular areas will have densities more than about twice as great at one *ED* detector as at the other. Those falling in the circle nearer the *PP* detector register penetrating showers six times as frequently as those falling in the other circle.

In the present experiment the requirement for all events is the detection of an N-component particle *and* one or more electrons. The mean distance to the cores of the showers is found to be about 5 to 10 meters. However, the mean distance of all nucleons from the shower cores may be 50–100 meters or more. In experiments where the detector only requires the presence of a single nucleon (as in almost all experiments on local penetrating showers), the associated shower cores will strike at an average distance so large that the associated air shower will usually not be detected. This can account for the usual observation[4,5,14–16] that N-component particles in the air occur without associated showers.

IX. IMPLICATIONS OF THE EXPERIMENTAL RESULTS

We have two properties to account for in the extensive air showers: (a) the existence of a large number of high energy nucleons, and (b) the concentration of the nucleons near the core of the shower. In showers that contain 10^7 electrons, there are about 50,000 nucleons of energy above several Bev, as well as[10] even more nucleons of lower energy. The concentration near the core is much like that of the electrons, for which the density function varies about as $1/r$ near the core.

From the large number of nucleons in the showers we may only conclude that the production occurs in a cascade, or succession of interactions, rather than in a single catastrophic event. Without more information, one cannot draw more detailed conclusions on the nature of the interactions involved. The production of many nucleons would be accomplished with greater efficiency if in each step of the cascade most of the energy is divided among a small number of high energy secondaries, rather than among a very large number. We cannot be sure, however, that this is the way it happens.

We may nowadays be fairly certain that a large part of the energy in each nuclear interaction is given to mesons, of which the neutral ones decay to produce the photons which generate the electronic part of the air showers. If the charged mesons have large cross sections for producing further nuclear interactions with further meson production, one can arrive at a consistent picture in which most of the energy, after 5 to 10 mean free paths, is transferred irreversibly to the electronic component, while 10 to 20 percent of the energy is distributed about equally between μ-mesons and nucleons. But if the charged mesons are supposed not to interact strongly with nuclei of the air such a consistent picture cannot be formed. In that case very few high energy nucleons would be produced and most of the energy of the shower would be retained by a rather small number of high energy mesons. Therefore we think it necessary to believe that the high energy charged mesons that are directly produced in nuclear interactions have a large cross section for nuclear interaction with further meson and nucleon production.

A direct inference that can be made from the spatial distribution is that a large fraction of the observed N-component originates locally in the core of the shower, within distances of the order of 200 meters of air (15 g/cm^2) above the apparatus.

For those particles which originate at a height greater than x above the apparatus, the spatial distribution about the core must be approximately flat within a distance of the order of $x\bar{\theta}$, where $\bar{\theta}$ is the average angle of divergence in the production process. For secondary nucleons of energy around 10 Bev, $\bar{\theta}$ must be at least as large as about 0.1 radian, hence the secondaries originating more than 200 meters above the apparatus must be expected to have a spatial distribution which is flat for lateral distances up to 20 meters, contrary to our observations. If the particles are π-mesons of about the same energy, the distance in which they must originate is limited to a few hundred meters by the decay probability. However, we suspect from the abundance of neutral particles in the N-component that most of the particles are nucleons.

Thus the N-component cascade in the extensive air showers must still be active in reproduction near the height of observation of the showers. The local activity, however, does not need to be as great as at higher altitudes.

Let x be the height above the level of observation of a shower, and $\rho(r)$ be the density of the N-component at a distance r from the core. Let $I(x)$ be the intensity of N-component production (per g/cm^2) in the core, and $f(\theta)$ be the angular distribution (per unit solid angle) of the secondaries. Then one can write

$$\rho(r)=K\int_{x=0}^{\infty}dx\left[\frac{x}{(x^2+r^2)^{\frac{3}{2}}}\right]f(\theta)I(x)\exp\left(-\frac{x}{x_0}-\frac{x}{\lambda}\right).$$

The term in brackets is just the solid angle subtended by a unit horizontal area at a height x. The term $\exp(-x/x_0)$ represents the decrease in density of the air, with $x_0\approx 7000$ m, while $\exp(-x/\lambda)$ represents absorption of the secondaries. Strictly, λ (in meters) should vary with the density of the air, but this is not impor-

tant here. λ, like x_0, is rather long—about 1700 meters for an absorption length of 130 g/cm². The equation neglects the production of high energy N-component by particles which are not in the core of the shower.

If the variation of the terms outside of the brackets is ignored, the purely geometric factor integrates to give $\rho(r) \propto r^{-1}$. This result is unchanged if the factor $f(\theta)$ is included, under the approximation

$$f(\theta) = \begin{cases} 0, & \theta > K, \\ \text{const.}, & \theta < K. \end{cases}$$

The main contribution to the particles at distance r from the axis is found to come from a height r/K to $2r/K$. Thus if $K = 0.1$ (particles in a cone of 6° half-angle), the particles found at 10 m from the core originate in the core mostly at heights of 100 to 200 meters.

The variation of $\rho(r)$ as r^{-1} is approximately the sort of variation that is necessary to account for our experimental data; a weaker dependence on r would not suffice.

The exponential terms in the above equation do not change much in distances of a few hundred meters, and therefore do not affect the dependence of ρ on r near the core.

Thus the only requirement needed to obtain the sort of lateral distribution which has been observed is that the intensity function $I(x)$ be finite and not vary too strongly with x. That is, one must be able to use the concept of a core that contains particles of enough energy to generate locally some particles of the N-component with secondary energies greater than 5 Bev. The number of such particles generated in the showers at mountain elevations must not be negligible compared with the numbers generated near the top of the atmosphere. However, an exponential increase of $I(x)$ with decreasing pressure, with a mean free path of the order of 100 g/cm², would be permissible.

The authors are grateful to the Research Corporation for a grant which covered the expense of performing the experiment described above. The facilities of the Inter-University High Altitude Laboratories were used in the performance of the experiment. We also wish to thank Professor Cocconi and Dr. Tongiorgi for helpful discussions of the experiment.